Chemical Physics Letters 589 (2013) 42–45

Contents lists available at ScienceDirect

Chemical Physics Letters

journal homepage: www.elsevier.com/locate/cplett

Reprint of: Femtosecond transition-state spectroscopy of iodine: From strongly bound to repulsive surface dynamics

R.M. Bowman, M. Dantus, A.H. Zewail

Arthur Amos Noyes Laboratory of Chemical Physics,[1] California Institute of Technology, Pasadena, CA 91125, USA

ARTICLE INFO

Article history:
Available online 21 August 2013

ABSTRACT

The application of femtosecond transition-state spectroscopy (FTS) to molecular iodine is reported. The real-time motion of wave packets prepared coherently in the bound B state is observed. In addition, the motion is probed near and above the dissociation limit for the reaction: $I_2 \rightarrow I\,(^2P_{3/2}) + I^*(^2P_{1/2})$. FTS measurements of the dynamics on repulsive surfaces are also reported.

1. Introduction

In femtosecond transition-state spectroscopy (FTS) [1] of reactions, the evolution of free fragments as they pass through transition states is probed at different interfragment separations (R). The wavelength of the probe pulse (λ_2) can either be in resonance with the free fragment transition (i.e. "infinite" separation R; λ_2^∞) or in tune with the transition state (i.e. fixed R; λ_2^*) [2]. In either case, the total energy available for the reaction ($E_{avl} = \frac{1}{2}\mu v_r^2$, where v_r is the recoil velocity) is determined by the wavelength (λ_1) of the initiation pulse. For a number of reactions this method of probing has resulted in the observation of the motion of the wave function (or wave packet) along unbound surfaces ("purely" repulsive) [1,3], quasi-bound surfaces (avoided crossings) [4], and multidimensional (vibrational) surfaces with a saddle point [5].

The study of halogens is of great interest because they exhibit the above characteristics (repulsive, quasibound and bound surfaces) in the various PES of their reactions:

$$X_2 \rightarrow X + X \text{ or } X_2 \rightarrow X + X^*.$$

They also were part of the very early study of crossed-beam reactions [6] and photon/molecular beam reactions [7], and connections with these studies will be valuable.

This Letter is concerned with FTS studies of iodine dissociation, and with the wave packet motion in the B state. By tuning λ_1, we observe very strong oscillatory behavior characteristic of the motion in the B state. From this temporal data we can deduce the spectroscopic constants. At other λ_1's we observe rapid decays (on the femtosecond time scale) that are characteristic of the "unbound" states which produce iodine atoms. By varying λ_2^* we probe different parts along R of the potential. The iodine molecule presents a unique opportunity for several reasons: (a) the bound and repulsive potentials have been assigned [8], (b) there is an abundance of spectroscopic information [9], and (c) iodine consists of two identical heavy atoms.

The idea of the experiment on iodine, together with an approximate display of the PESs, are outlined in Fig. 1. A pump pulse (λ_1) prepares a coherent wave packet in any of three regions: (a) on a repulsive PES, (b) on a bound PES, or (c) in the continuum (or quasicontinuum) states where dissociation occurs. The probing of the dynamics in the three regions is carried out by the second pulse (λ_2) which takes the coherently prepared wave packet into an upper fluorescent state. The observed signal is a plot of the probe-induced fluorescence as a function of the time delay between the pump and probe lasers. One major advantage of this scheme is the ability to probe at short R's because of the involvement of a bound "fluorescent" state at λ_2^*. This is similar to the earlier case [10] where multiphoton ionization was utilized to probe dissociation on repulsive surfaces but with the probe tuned to a bound ion state to restrict the range of R.

2. Experimental

The experimental apparatus has been described in detail elsewhere [3–5]. Briefly, the system consists of a CPM laser amplified by a Nd:YAG laser. These amplified pulses have an energy of up to 0.3–0.5 mJ and a pulsewidth (fwhm) as short as 50 fs. Nonlinear techniques (e.g. frequency doubling, sum frequency mixing with the YAG wavelengths and continuum generation) were used to generate the necessary colors for the experiments. All the pulses were spectrally and temporally characterized, and attenuated to insure linearity (or near linearity) of the power dependence. Cross-correlations of 80–90 fs were obtained for the experiments involving the ≈ 390 nm mixed light. The iodine was kept in a slow flow fluorescence cell at low pressures (<100 mTorr) at room temperature.

[1] Contribution No. 8016.

0009-2614/$ - see front matter © 2013 Published by Elsevier B.V.
http://dx.doi.org/10.1016/j.cplett.2013.08.065

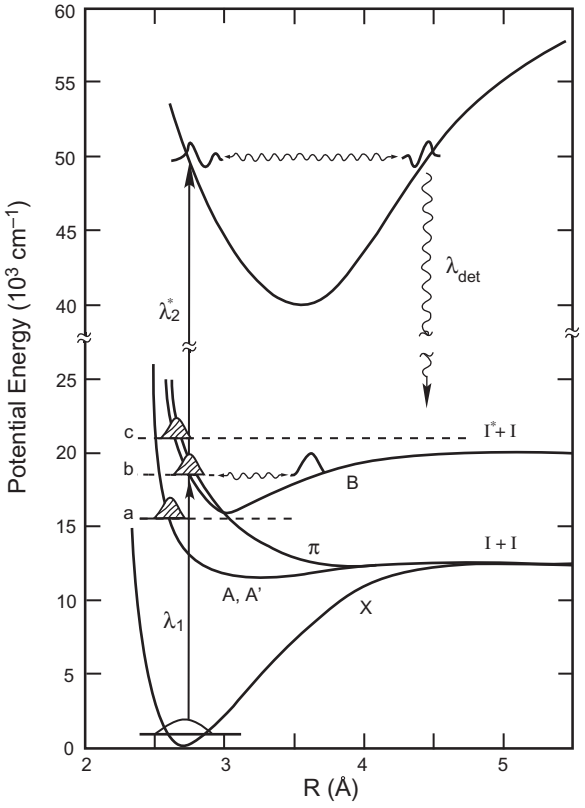

Fig. 1. Schematic (approximate) of the bound and repulsive potential energy surfaces relevant to the FTS study of iodine. The states are labelled briefly, and grouped in accordance with previous spectroscopic work (see text).

3. Results and discussion

3.1. Bound state dynamics

Fig. 2 shows a typical transient obtained for a pump wavelength of 620 nm and a probe wavelength of 310 nm detecting the fluorescence at the well known emission (see Fig. 1) near 340 nm following single and two photon excitation [8,11]. In the notation of previous publications [5] we designate this transient $\lambda_1/\lambda_2^*(\lambda_{det})$ in nm = 620/310 (340). This transient consists of strongly interfering oscillations. Since the femtosecond pulse duration is shorter than the vibrational period of I_2, the pump prepares the B state of iodine in a coherent superposition of a few vibrational states (determined by the bandwidth of the pulse and the slope of the repulsive surface). Thus, the signal is clearly the result of the interferences between the vibrational levels excited. The short time oscillation (300 fs) is the period of the wave packet motion at this particular energy. It can be directly related to the vibrational levels excited. In this case, λ_1 = 620 nm and the B state is prepared around v' = 3. Using the spectroscopic parameters of I_2 [12], we obtain a vibrational spacing of 122 cm^{-1}, which translates to a period of 273 fs. Better agreement with the experimentally obtained periods is achieved when the initial thermal energy is taken into account; the absorption from the different v'' states is known at the wavelengths studied [12]. Also, the measured period (T_a) is obtained from direct peak to peak measurement and not from complete analysis of the waveform. The shape of the oscillatory transient in the top of Fig. 2 can easily be simulated using the conditions of our experiments; the behavior is described simply by the motion of, for example, two wave packets that start in phase and rephase at later times determined by the difference of their frequencies. This analysis together with a Fourier transform treatment of the data will be published elsewhere when these studies are completed.

Keeping the probe wavelength fixed at 310 nm and varying the pump wavelength within the bound portion of the B state (634–500 nm), i.e. starting at different points in the vibrational manifold, we observe different periods in the coherent evolution of wave packets. Fig. 3 shows a selection of the transients we have recorded where the period of oscillation is shown to increase as the pump energy is increased, i.e. motion starting at higher vibrational levels.

The transients in Fig. 3 show oscillations with an average period of 750, 500 and 290 fs for the top (this transient shows an irregular oscillation pattern at times longer than shown), middle and bottom transients, respectively. Calculation of these oscillation periods has also been made using the available spectroscopic information of the B state, and good agreement was found between the calculated and observed periods as a function of excitation energy. In the future we will use the data to deduce characteristics of the potential surface in the region of dissociation to I + I*.

In order to confirm that the oscillations are due to the wave packet prepared by the pump pulse, we used a different probe pulse at 390 nm. In this case the fluorescence maxima occurred at 426 nm, known as the E → B transition [13]. The bottom of Fig. 2 shows a typical 620/390 (426) transient where the short time oscillation period is the same as that of the 620/310 (340) transient, i.e. 300 fs. It should be noted that the depth of modulation and envelope decay are different for the two probe wavelengths. This can be related to the position in the well where the Franck–Condon overlap with respect to the probe pulse is maximized, and this will be analyzed in our forthcoming study.

The measured oscillations of the wave packet prepared in this fashion last for longer than 40 ps. There is no sign of decay of the total signal since the lifetime of the B state is very long (microsecond time scale) compared to the femtosecond time scale of these experiments. However, the envelope of the transients decays on a shorter time scale (see Fig. 2) and this reflects the coherence decay dictated by the preparation process and the spread of the packets.

3.2. Repulsive versus bound surfaces

In the previous section the pump pulse accessed states within the bound portion of the B state PES and showed well behaved oscillations. We now turn to experiments where the pumping is into the continuum levels above the dissociation limit to I + I* (higher energies), and pumping into known repulsive states at lower energies than the B state. These data are shown in Fig. 4.

The top transient in Fig. 4 was obtained by pumping at 700 nm. The absorption spectrum of I_2 can be resolved into three regions for the three states involved: $^1\Pi_{1u}$ (blue absorption), $B^3\Pi_{0u}$ and $A^3\Pi_{1u}$ (red absorption) [12]. The bottom of the B state well corresponds to 634 nm, and the absorption at 700 nm, therefore, is due to the A state and some hot band absorption to the B state [12]. The 700/310 (340) transient shows a rise and decay typical of FTS off-resonant probing. When the latter part of the transient is expanded (×5), oscillations with a period of 250 fs are seen (the amplitude of the oscillating portion of the signal corresponds to ≈ 5% of the total signal). Near the bottom of the B state this period is expected. The observed FTS transient, therefore, reflects the dynamics in this region for both the A and B states.

Tuning the pump laser to lower energies minimizes the overlap with the B state. The transient, 750/310 (340) (not shown) displays totally FTS off-resonance behavior as has been discussed in great detail in previous works [1–5]. The signal shows a rise and decay much like the 700/310 (340) data at the top of Fig. 4, but the signal decays to zero amplitude showing no oscillatory behavior. The information contained in this transient corresponds to the

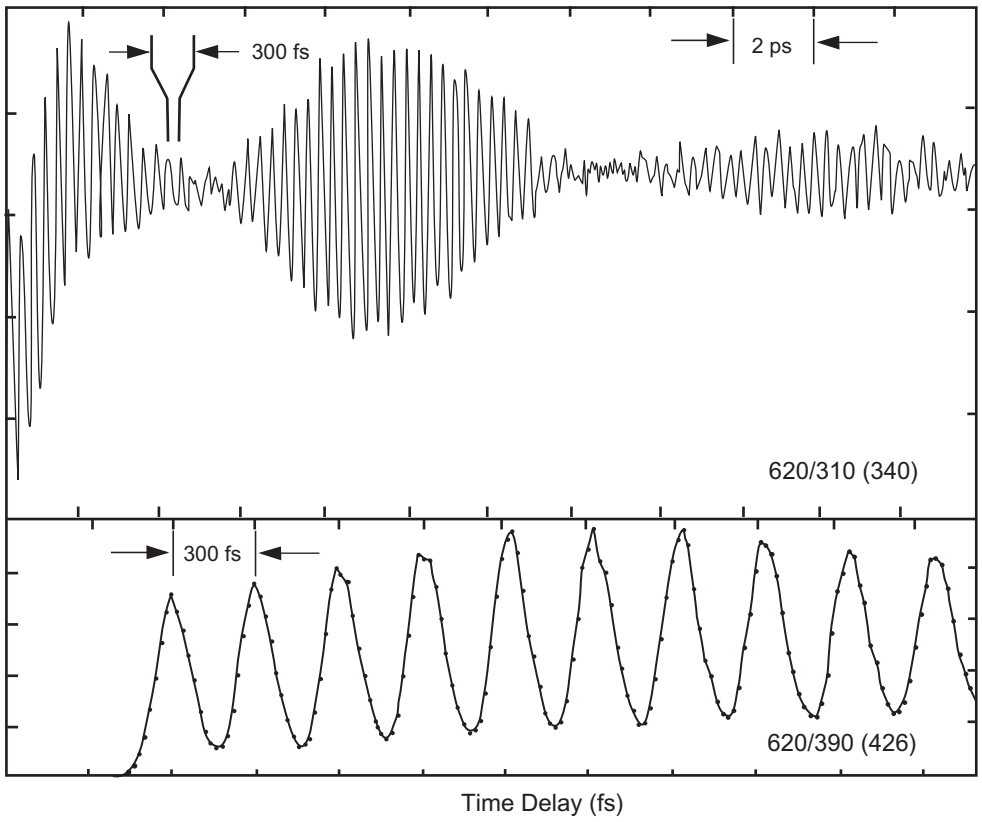

Fig. 2. Top: Typical FTS transient obtained for 620/310 (340) showing the wave packet dynamics in the strongly bound B state. Bottom: Typical FTS transient, 620/390 (426), showing the period of oscillation to be invariant with the probe wavelength. Note that the time scales are different for the two transients.

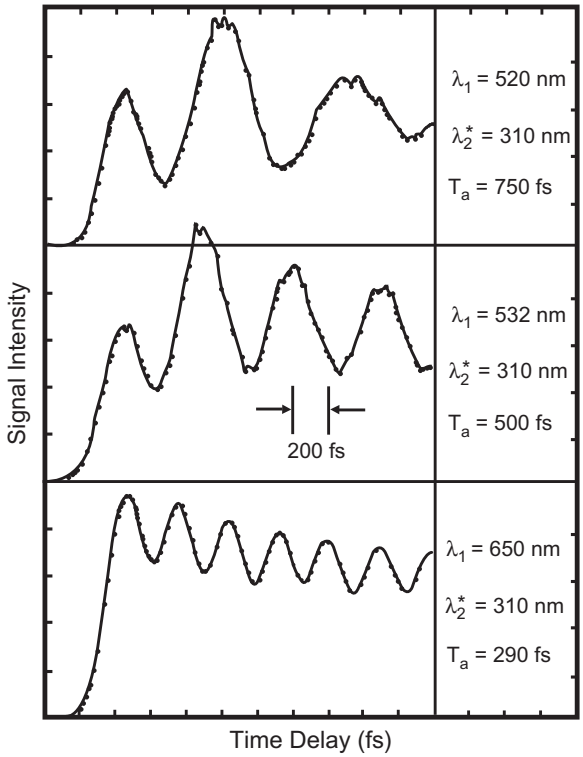

Fig. 3. FTS transients obtained at different pump laser wavelengths (λ_1). The time scale for the three traces is the same (200 fs/division). The periods are measured peak to peak between the second and third oscillations in order to avoid convolution effects. Complete analysis of these transients will give better values (see text).

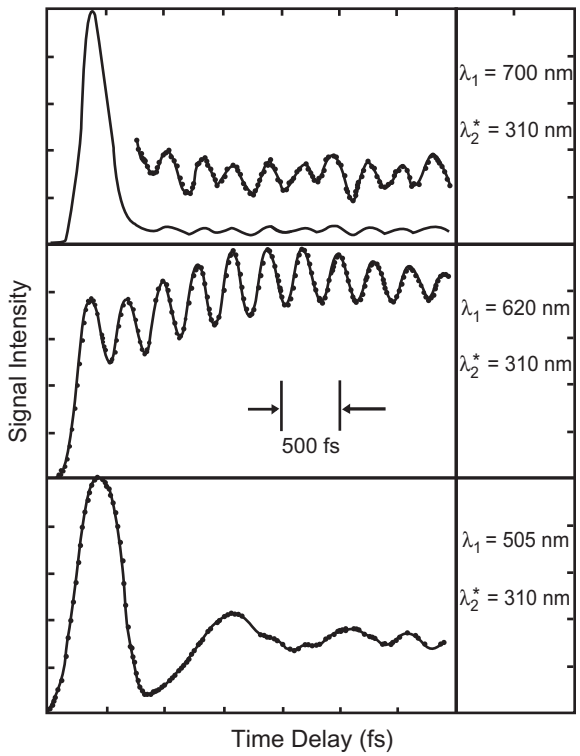

Fig. 4. FTS transients obtained using different pump energies spanning repulsive and bound states. Top: Transient corresponding to case (a) type in Fig. 1. At long times the oscillatory behavior is displayed. Middle: Transient obtained from strongly bound B state (see Fig. 1). Bottom: Transient showing the time evolution of a wave packet near the B state dissociation limit.

evolution of the wave packet at very short *R*'s in the Franck–Condon region, and we are in the process of analyzing the time-dependent shape.

The upper limit of the B state presents a different opportunity to explore dissociative states but this time the continuum or quasicontinuum states (case (c) in Fig. 1). In addition the $^1\Pi$ has an absorption at these higher energies. Tuning the pump wavelength to 505 nm we obtained the transient shown in the bottom of Fig. 4. Unlike the transients in Fig. 2 or the transient in the middle of Fig. 4, this transient shows a very large signal at early times and damped oscillations. From the latter portion of the 505/310 (340) data it is concluded that some fraction of the wave packet is reflected and returns to the probing region after ≈1.2 ps. The highly anharmonic vibrational levels of the B state ($v' \approx 50$) gives a period similar in value.

The reflected portion of the wave packet corresponds to the quasicontinuum states overlapped by the pump laser. Tuning to higher energies (490 nm) insures no bound states are overlapped and no wave packet reflection is observed. The 490/310 (340) transient (not shown) simply displays FTS off-resonance-like behavior, which in this case is a combination of both the continuum B state and the purely repulsive $^1\Pi$ state dynamics.

From these transients at different λ_1 and λ_2^*, characteristics of these PESs can be deduced in the bound and dissociative regions. The transients shown in Figs. 3 and 4 are ideal for the inversion method given in Ref. [14]. In fact, the data in Fig. 4 (bottom) are reminiscent of the expected behavior [14] for FTS observations on a repulsive surface with a well. This analysis will be given elsewhere.

Finally, as for the FTS experiments of HgI_2 [5], we have observed polarization anisotropy decays on the femtosecond time scale for I_2, and this should give the alignment information, similar to that obtained in Ref. [5]. In this case, analysis of the alignment in real-time will give a comparison of the rotational (angular) dephasing time to the scalar wave packet dynamics, i.e. the period of oscillation or the dissociation time. In all experiments reported here the relative polarization was fixed at perpendicular.

4. Conclusions

The application of FTS to molecular iodine has allowed us to observe the real-time motion of wave packets prepared coherently in a bound, quasicontinuum or repulsive state. For the B state, FTS shows that the wave packet moves in the well, and dephases and rephases with well-defined time constants, directly related to the vibrational energies and anharmonicity. Since the spectroscopy of I_2 is well known, comparisons with the B state potential are made. By tuning the pump wavelength to the red of the potential minimum and to the blue of the dissociation limit we were able to probe the dynamics on both a dissociative potential and in the continuum levels of a bound PES. In all of these cases the probing was done in the region of small interfragment separation (*R*) accessed in the Franck–Condon region of the pump pulse. Probing at larger *R* will involve the detection of iodine atoms as done in other FTS studies [1–5]. In progress are experiments on other halogens and interhalogens [15]. We are also performing condensed phase experiments to understand the influence of solvation on these bound and unbound systems using FTS.

Acknowledgement

This work was supported by a grant from the Air Force Office of Scientific Research.

References

[1] M. Dantus, M.J. Rosker, A.H. Zewail, J. Chem. Phys. 87 (1987) 2395.
[2] A.H. Zewail, Science 242 (1988) 1645;
A.H. Zewail, R.B. Bernstein, Chem. Eng. News 66 (1988) 24;
J. Bagott, New Scientist 1669 (1989) 58.
[3] M.J. Rosker, M. Dantus, A.H. Zewail, J. Chem. Phys. 89 (1988) 6113;
M. Dantus, M.J. Rosker, A.H. Zewail, J. Chem. Phys. 89 (1988) 6128.
[4] T.S. Rose, M.J. Rosker, A.H. Zewail, J. Chem. Phys. 88 (1988) 6672;
M.J. Rosker, T.S. Rose, A.H. Zewail, Chem. Phys. Letters 146 (1988) 175;
T.S. Rose, M.J. Rosker, A.H. Zewail, J. Chem. Phys. 91 (1989) 7415.
[5] R.M. Bowman, M. Dantus, A.H. Zewail, Chem. Phys. Letters 156 (1989) 131;
M. Dantus, R.M. Bowman, J.S. Baskin, A.H. Zewail, Chem. Phys. Letters 159 (1989) 406;
M. Dantus, R.M. Bowman, M. Gruebele, A.H. Zewail, J. Chem. Phys 91 (1989) 7437.
[6] D.R. Herschbach, Faraday Discussions Chem. Soc. 55 (1973) 233;
R.N. Zare, D.R. Herschbach, Proc. IEEE 51 (1963) 173;
R.N. Zare, D.R. Herschbach, Appl. Opt. Suppl. 2 (Chemical Lasers) (1965) 193.
[7] G.E. Busch, R.T. Mahoney, R.I. Morris, K.R. Wilson, J. Chem. Phys. 51 (1969) 837;
R.J. Oldman, R.K. Sander, K.R. Wilson, J. Chem. Phys. 54 (1971) 4127;
R.W. Diesen, J.C. Wahr, S.E. Adler, J. Chem. Phys. 50 (1969) 3635.
[8] R.S. Mulliken, J. Chem. Phys. 55 (1971) 288;
J.C.D. Brand, A.R. Hoy, Appl. Spectry. Rev. 23 (1987) 285.
[9] J.I. Steinfeld, R.N. Zare, L. Jones, M. Lesk, W. Klemperer, J. Chem. Phys. 42 (1965) 25;
R.J. LeRoy, R.B. Bernstein, J. Mol. Spectry. 37 (1971) 109;
M.D. Danyluk, G.W. King, Chem. Phys. 25 (1977) 343;
A.L. Guy, K.S. Viswanathan, A. Sur, J. Tellinghuisen, Chem. Phys. Letters 73 (1980) 582.
[10] L.R. Khundkar, A.H. Zewail, Chem. Phys. Letters 142 (1987) 426.
[11] H. Hemmati, G.J. Collins, Chem. Phys. Letters 75 (1980) 488;
U. Heeman, H. Knöckel, E. Tiemann, Chem. Phys. Letters 90 (1982) 17;
J.C.D. Brand, A.R. Hoy, Can. J. Phys. 60 (1982) 1209;
H.P. Grieneisen, R.E. Francke, Chem. Phys. Letters 88 (1982) 585.
[12] J. Tellinghuisen, J. Chem. Phys. 58 (1973) 2821;
P. Luc, J. Mol. Spectry. 80 (1980) 41;
S. Gerstenkorn, P. Luc, Atlas du spectre d'absorption de la molécule d'Iode, CNRS, Paris, 1978;
R.B. Snadden, J. Chem. Educ. 64 (1987) 919.
[13] D.L. Rousseau, P.F. Williams, Phys. Rev. Letters 33 (1974) 1368;
D.L. Rousseau, J. Mol. Spectry. 58 (1975) 481;
M.D. Danyluk, G.W. King, Chem. Phys. 22 (1977) 59;
S.L. Cunha, J.A. Lisboa, R.E. Francke, H.P. Grieneisen, Opt. Commun. 28 (1979) 321;
G.W. King, I.M. Littlewood, J.R. Robins, Chem. Phys. 56 (1981) 145;
J.C.D. Brand, A.K. Kalukar, A.B. Yamashita, Opt. Commun. 39 (1981) 235.
[14] R.B. Bernstein, A.H. Zewail, J. Chem. Phys. 90 (1989) 829.
[15] M.S. Child, R.B. Bernstein, J. Chem. Phys. 59 (1973) 5916;
J.C.D. Brand, A.R. Hoy, Appl. Spectry. Rev. 23 (1987) 285.